Nanotube Self-Assembly of a Styrene and Maleimide Alternating Copolymer

Thomas D. Lazzara,[†] Theo G. M. van de Ven,*[,‡] and M. A. (Tony) Whitehead[†]

Department of Chemistry, McGill University, 801 Sherbrooke St. West, Montreal, Quebec H3A 2K6, Canada, and Department of Chemistry, Pulp and Paper Research Centre, McGill University, 3420 University St., Montreal, Quebec H3A 2A7, Canada

Received April 25, 2008; Revised Manuscript Received July 10, 2008

ABSTRACT: The self-assembly of poly(styrene-*alt*-dimethyl-*N,N*-propylamide) (SMI) polymers into nanotubes was studied using semiempirical PM3 calculations. Ordered polymer self-assembly results from π-stacking of styrenes and van der Waals interactions between the maleimide chains. Every styrene, and half of the maleimide chains, in a racemo-di-isotactic SMI polymer form π-stacks and chain−chain pairs with neighboring racemo-di-isotactic polymer. Racemo-di-isotactic polymers in bent associations form a minimum-energy nanotube structure. Nanorods were observed experimentally with diameters of ∼5 nm.

Introduction

Nanotubes are hollow curved architectures with diameters in the nanometer range but with varying lengths. Organic nanotubes[1−8] are of interest because of their versatile use as templates and because they can be chemically modified to create new functional materials.[9−12]

Poly(styrene-*alt*-maleic anhydride) (SMA) is a polymer with alternating hydrophobic and hydrophilic monomers. Its unusual composition gives it properties that have been used in many nanotechnology applications[13−19] and in drug delivery.[20,21] Hydrolyzing maleic anhydride of SMA to succinic acid allows self-assembly into nanotubes, at 50% protonation.[18] At these conditions, the polymers are linear because of multiple intrapolymer H-bonds in the succinic acids, stiffening the polymer, which increases its persistence length.[22]

A derivative of SMA was studied to modify of the size and shape of the nanotube. Poly(styrene-*alt*-dimethyl-*N,N*-propylamide) (SMI, Figure 1) is soluble in acidic aqueous solution. The chosen alternating copolymer retains the styrene monomers for π-stacking interactions responsible for SMA nanotube formation, and the maleic anhydride is functionalized to a maleimide. We recently performed calculations on the conformation of SMI and showed that, because of the stiffness of the maleimide, only racemo-di-isotactic polymers have ordered styrenes and therefore self-assemble.[23] In the present paper, the association between multiple polymers is modeled using this chirality. Experimental characterization of the self-assembly was investigated using AFM and TEM.

Materials and Experimental Methods

Material. Low molecular weight SMI 1001 was purchased from Sartomer Inc. This copolymer is prepared from low molecular weight SMA polymer (M_w 1600) and *N,N*-dimethylpropylamine.

Instruments. The pH was measured using an Accumet Basic AB15 (Fisher Scientific). AFM scans were acquired in noncontact mode using SiN tips purchased from Veeco on a Digital Instruments NanoScope IIIA. TEM measurements were performed on a JEOL JEM-2000FX 200 kV, operated at 80 kV. TEM size analysis was performed using SigmaScan Pro (version 4). AFM images analysis was performed using the NanoScope version, 6.13r software.

* Corresponding author: Tel 514-398-6177; Fax 514-398-8254; e-mail theo.vandeven@mcgill.ca.
[†] Department of Chemistry.
[‡] Department of Chemistry, Pulp and Paper Research Centre.

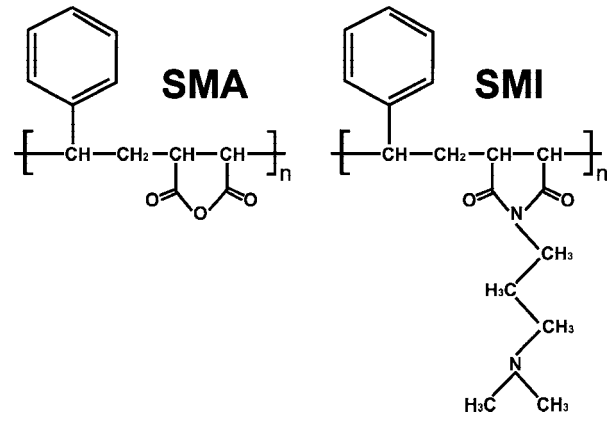

Figure 1. Chemical structures of SMA and SMI polymers.

Solution Preparation of SMI Nanotubes. The polymer resin was dispersed in deionized water, filtered using 0.2 μm PTFE filters (Sigma-Aldrich, Acrodisc CR syringe filters) at a concentration of 1 wt %. Deionized water was obtained from a Millipore ion exchange filtering unit equipped with an activated carbon cartridge. The suspension was brought to pH 3 by slow addition of HCl standard 1 N solution, also filtered. The acid was added until the polymer was completely dissolved. Only racemo-di-isotactic polymers are expected to form nanostructures, and because each monomer has three chiral centers, yields are expected to be low, as observed. The nanotubes could still be observed because the nanostructures are much larger than nonassociated polymer and have an ordered structure and can therefore be distinguished from nonassociated polymer. The SMI sample used is approximately an octamer with a contour length of 4 nm. The percentage of racemo-di-isotactic polymer in the commercial product is not known but expected to be low.

Dynamic Light Scattering. Organic solvents used were HPLC grade. The solutions of polymer dissolved in organic solvent and water, 1 wt %, were filtered using 0.2 μm filters. The Contin model was used to obtain particle size distribution. The polystyrene standard used was from Duke Scientific with particle diameter of 100 nm. The angular scans of the polystyrene standard and the SMI solution, both prepared from filtered deionized water, were acquired from 20° to 80°. Measurements were performed on a Brookhaven Instrument system equipped with the BI 2030 digital correlator and a 25 mW He−Ne (632.8 nm) at a temperature of 21 °C.

Sample Preparation. For AFM imaging, 200 μL of pyrrole was added to 10 mL of SMI solution and left to interact with the

10.1021/ma800926a CCC: $40.75 © 2008 American Chemical Society
Published on Web 08/21/2008

nanotubes under acidic conditions. Addition of pyrrole was used to stabilize the SMA nanotubes by filling the gaps present inside and around the nanotube through possible H-bonding and hydrophobic stabilization in areas where pyrrole can concentrate and polymerize under acidic conditions. The poly(pyrrole) acts as a stabilizing filler.[19,24] This approach, used successfully for SMA, was therefore used to stabilize the SMI nanostructures. A drop of the SMI polymer nanotube solution was deposited on the mica surface and left for 5 min, and the excess liquid was removed by a filter paper. The sample was rinsed with a drop of water. TEM samples were prepared by depositing the solution onto a carbon-coated grid (400 mesh from SPI) and left to rest for 2 min, and the excess liquid was adsorbed using a Kemwipe.

Theoretical Methods. The association between SMI polymers was modeled using SMI hexamers. Linear associations between SMI polymers were previously studied.[23] We present new additional calculations on bent associations and have included previous results for comparison. Semiempirical PM3 caculations were used as described previously.[23] The stabilization energy and stacking geometry of the styrenes agree with results for similar systems.[25−27] All calculations were performed using the Gaussian 03 program.[28]

Interactions between SMI Polymers

π-Stacking interactions between styrenes and the van der Waals forces between maleimide chains cause SMI polymer aggregation. Racemo-di-isotactic SMI polymers have an ordered distribution of styrenes along a main axis, with maleimide chains at 70° to the styrenes. In contrast, atactic polymers structures are not periodic, preventing ordered association.[23] We found two possible association conformations: head-to-tail in which the polymers are in identical orientations and head-to-head where they are in opposite orientations.[23] SMI polymers can join with different association angles, and three limiting geometries exist: when there is no rotation between polymers (linear association) and two limiting cases if the rotation is ±60° (bent associations). Association distances and stabilization energies have been previously calculated for the linear associations 2 and 5 using a series of constrained optimizations, followed by relaxing the system.[23] Here, the associations 1, 3, and 4 = 6 are calculated using the methods for 2 (Figure 2).

Evaluating the energy as a function of inter-phenyl distance (r') allows comparison of the six associations (Figure 3). The average r' is between 4.2 and 5.5 Å. The bent associations 1, 3, 4, and 6 are the most stable, with ~20 kJ/mol of stabilization energy for each π-stacking monomer pair (for two hexamers, there are three π-stacking pairs). Figure 3 summarizes the PM3 results obtained when the constraints are released. The stabilization energy from π-stacking was previously determined by the same type of calculation on the linear association complexes 2 and 5.[23] Chain−chain interactions are negligible for linear associations, and the stabilization energy represents only π-stacking: 13 kJ/mol per π-stack. The increased stabilization energy for bent associations compare to linear ones comes from chain−chain stabilizing van der Waals interactions between the maleimide chains, and this contributes about 7 kJ/mol per monomer pair. Both π-stacking and van der Waals interactions are present in bent associations and produce more stable complexes than linear ones. If maleimide chains are shorter, the stabilization energy for bent associations does not change much compared to linear ones. Complexes with no chain−chain interactions would become insensitive to changes in association angles.

Nanotubes from Self-Assembled SMI Polymers

Associations beyond two hexamers (about 500 atoms) could not be investigated computationally. The optimal inter-phenyl distances and association angles from the most stable bent associations were used to build larger complexes. The inter-phenyl distance is about 5 Å with association angles of 60°. The bent association (1, 3, 4 = 6) are energetically equivalent and therefore equally probable, leading to polymer sheets, formed from combinations of bent associations and grown by addition of racemo-di-isotactic polymers. As sheets grow, nonassociated peripheral styrenes remain, and the system is more stable if additional π-stacks form between peripheral styrenes. The curvature required to form a closed tube does not come at the expense of steric constraints because the bent associations already form a 60° angle. In a closed loop, the hydrophobic styrenes and half of the maleimide chains are no longer in contact with the hydrophilic solvent, but interact within a more hydrophobic environment, inside the nanotube walls. This gives a closed octagonal structure consisting of eight SMI polymers forming a short polymer nanotube segment. Figure 4 shows an SMI nanotube from eight polymers in the head-to-head conformation. The inter-phenyl distances and association angles from the optimized values were used to build the 3-dimensional nanotube. Using different periphery atoms as measurement

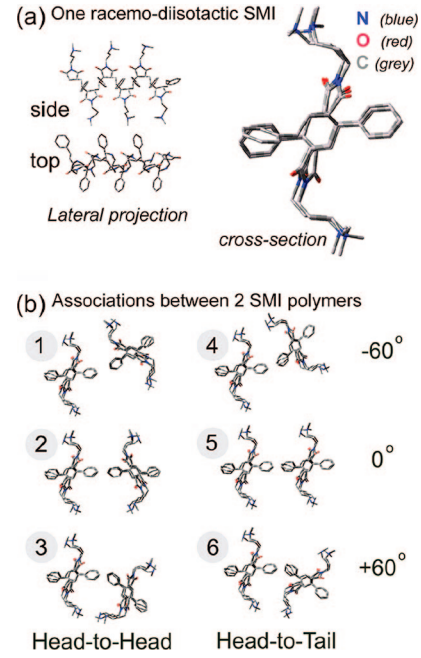

Figure 2. (a) Lateral and cross-section view of a racemo-di-isotactic SMI polymer[23] (hydrogens removed for clarity). (b) The six associations studied: 2, 5 are linear and 1, 3, 4, 5 are bent associations. Associations 4 and 6 are equivalent, and associations 2 and 5 have been studied previously.[23]

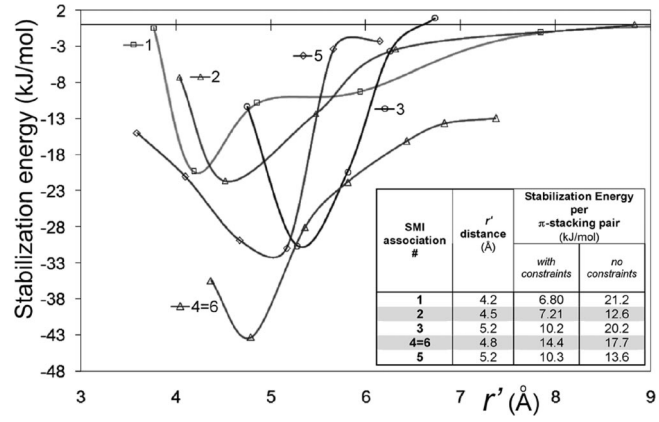

SMI association #	r' distance (Å)	Stabilization Energy per π-stacking pair (kJ/mol)	
		with constraints	*no constraints*
1	4.2	6.80	21.2
2	4.5	7.21	12.6
3	5.2	10.2	20.2
4=6	4.8	14.4	17.7
5	5.2	10.3	13.6

Figure 3. Stabilization energy as a function of r' for the different associations. The stabilization energies are given for two hexamers and therefore for three π-stacking SMI styrene pairs. Inset table: PM3 results for r' and energies calculated with constraints and after their release.

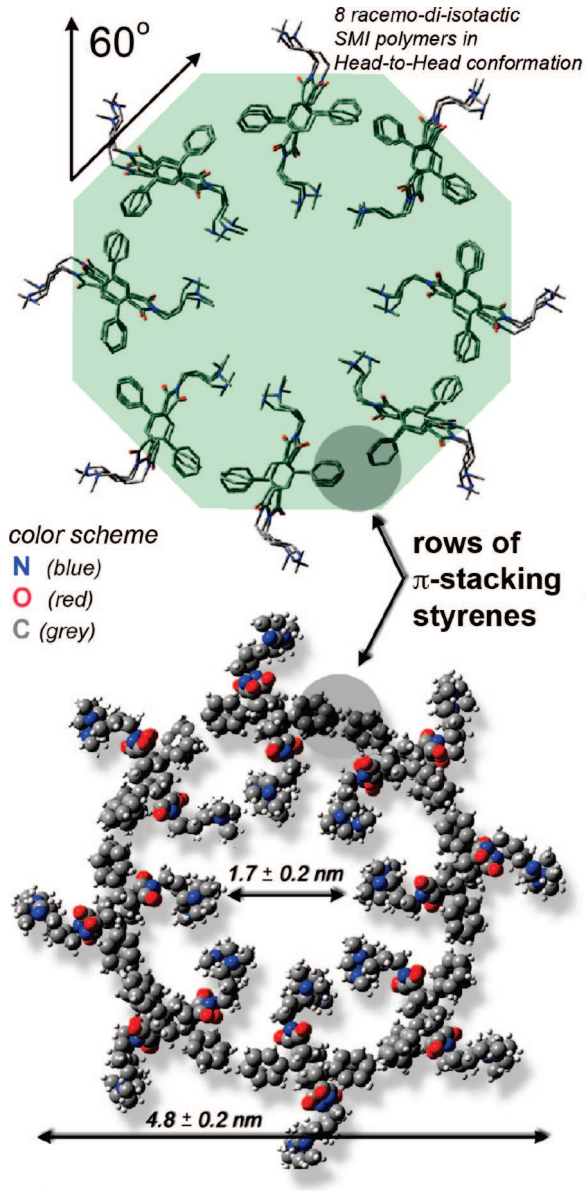

Figure 4. SMI nanotube (cross section, perpendicular to association plane): (top) the nanotube has an octagonal shape, made from eight racemo-di-isotactic SMI polymers in the head-to-head conformation; (bottom) SMI nanotube shown with van der Waals radii.

reference points gave an outer diameter of 4.8 ± 0.2 nm and an inner diameter of 1.7 ± 0.2 nm. An equivalent structure is also possible for SMI polymers associating in a head-to-tail conformation and a mixture of the two conformations. Stabilization energies, inter-phenyl distances, and association angles are comparable between head-to-head and head-to-tail conformations. The nanotube forms only by association of racemo-di-isotactic polymers.

Because polymers are typically polydisperse, and π-stacking is rarely perfect between associated polymers, the short closed segment can have protruding polymers. These ends offer nucleation points where addition of further racemo-di-isotactic polymers occurs. The nanotube linear growth is illustrated in Figure 5. SMI nanotubes are not expected to associate in bundles, as was the case for SMA nanotubes, but to remain as individual rods. All the styrenes π-stack inside the walls of the nanotubes and are therefore unavailable for further interaction between nanotubes. Unfavorable solvent−styrene interactions are decreased, and favorable hydrophobic styrene−styrene and

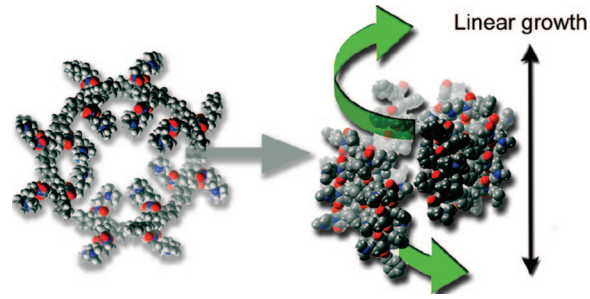

Figure 5. Proposed linear growth mechanism for SMI nanotubes. SMI polymers self-assemble at the edges of an initially closed structure, and the addition makes the nanotube grow in length (arrows) (lighter shade atoms are further behind the plane of view).

chain−chain interactions are increased in polar solvents such as water.

Experimental Characterization

Non-contact mode AFM was performed on the SMI nanotube solution deposited on a mica surfaces to investigate the size and shape of the self-assembled nanostructures. Mica was chosen because the atomically flat surface, which can provide improved imaging of small features. The SMI nanotubes were left to interact with pyrrole in acidic environment (pH 3). AFM results showed that a large fraction of the polymer had an amorphous structure, seen from the large amount of polymer deposited as an amorphous film. The mica surface was rarely visible and covered by nonassociated polymer. The amorphous layer appears as a *soft* surface when scanned (Figure 6). Some areas presented wormlike to rodlike features, which originate from ordered nonrigid self-assembly of SMI polymers. These structures were not present in the control solution containing the same amount of pyrrole at the same pH in deionized water. The average height of the rods measured by scanning across the nanotube was found to be between 4.5 and 5 nm (inset, Figure 6). The structure along the wormlike rod is nonuniform most likely because of nonuniform pyrrole polymerization, which also increases the apparent diameter (but not the height). The nanotube lengths are ~50 times greater than the polymer contour length. The branching observed is a result of defects in the self-assembly: tubes continue to grow from bifurcation points. These structures do not aggregate and remain as individual nanotubes because there is no driving force for aggregation.

The TEM investigation revealed short polymer rods (Figure 7). Here, the SMI nanotubes were studied without pyrrole because poly(pyrrole) also polymerizes freely in solution, which leads to various artifacts, and also because poly(pyrrole) and the SMI polymer have similar electron densities. Because the percentage of nanotubes is very low, imaging with the conditions used in AFM did not produce distinguishable samples. The observed nanotubes were shorter in length than those observed by AFM because of the absence of pyrrole, which helps stabilize the structure. The nanorods had a cross-section diameter of 6.5 ± 1.5 nm and agree, within experimental error, with the predicted dimensions.

The experimental TEM nanotubes diameter was 6.5 ± 1.5 nm and 4.5−5 nm from AFM, which agrees with the predicted dimensions of the outer diameter obtained from molecular orbital theory modeling. DLS was performed on the SMI nanotube solution at pH 3. The characteristic width of the intensity spectra (Γ) is proportional to the translational diffusion coefficient (D_T) and the square of the scattering vector (q^2). This is valid for isotropic scattering elements, such as spheres, and is independent of scattering angle. However, if the scattering element is anisotropic, an additional correction to Γ is required.[29] The

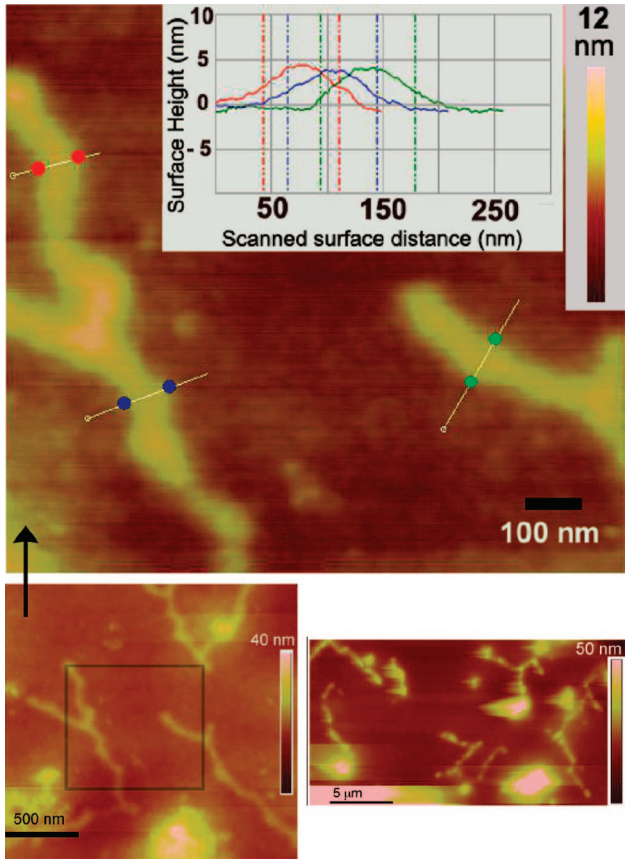

Figure 6. AFM of SMI nanorods on mica. The surface is covered with nonassociated polymer. Top inset: three different height profiles taken along 100−250 nm distances showing the height of the SMI nanotubes (shown on AFM scan). The linear features are nonrigid SMI nanotubes. The average height is about 4.5 nm.

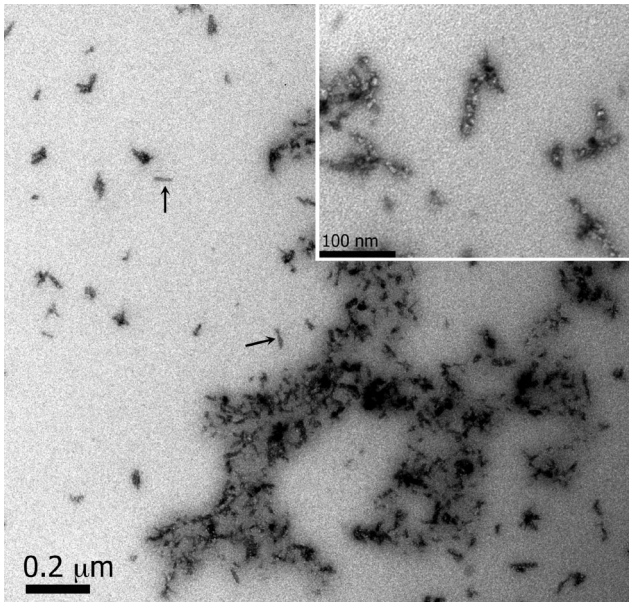

Figure 7. TEM of SMI, pyrrole was not added. Needle structures (arrows) are observed with diameters comparable to AFM measurements, but shorter. The average cross-section diameter is 6.5 ± 1.5 nm. Inset: enlarged view of a needle structure (beginning to decompose under electron beam).

hydrodynamic radius of the SMI polymer in aqueous solution shows aggregates about 20 times larger than the particles present in organic solvents: acetonitrile, ethanol, and methanol. A trend is observed: when the dielectric constant increases, larger

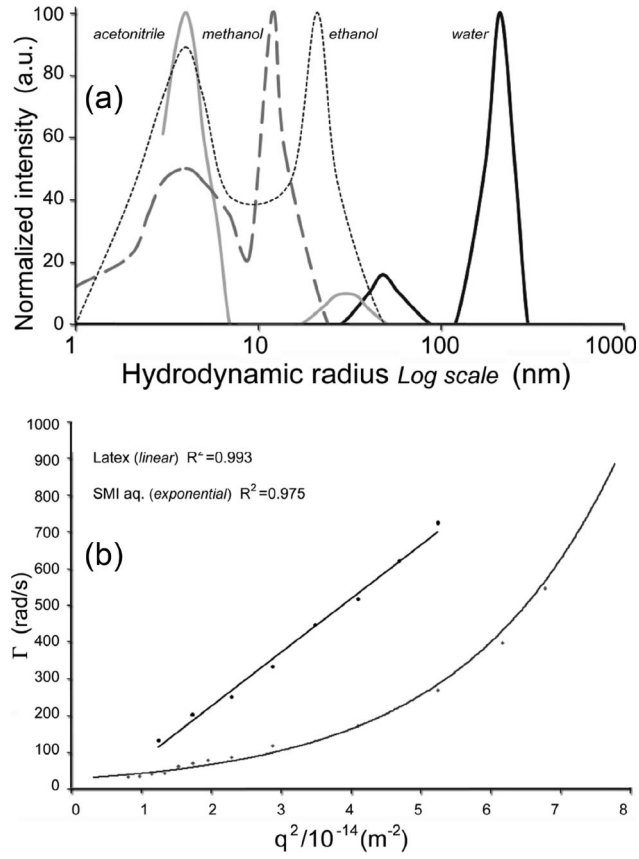

Figure 8. (a) DLS of SMI solution at pH 3. Particle size distributions determined using the Contin model, for SMI polymer dissolved in different dielectic constant solvents. (b) Low-angle DLS measurements of a 100 nm standard spherical latex particles and SMI pH 3 solution. The exponential fit of the SMI data indicates that a fraction of the particles are anisotropic.

aggregates are observed: methanol ∼ ethanol < acetonitrile < water. Aggregation in the organic solvents is limited to about 10 nm, consisting of a few polymers, at most, while water shows aggregates of around 170 nm. There is also this double distribution in both organic solvents and water. This may be due the existence of disordered small aggregates and larger ordered aggregates, SMI nanotubes.

Because the nanostructures are polydisperse and unassociated polymer is in excess, an exact value for the axis ratio could not be determined by DSL. However, particle size distribution in different solvents and the anisotropy were studied. The autocorrelation function of the scattered light intensity−time fluctuations $g(\tau)$ provides the characteristic width of the intensity spectra (Γ). For spherical scattering elements, Γ follows a linear relation with q^2. An exponential dependence on q^2 is expected for anisotropic particles such as those formed from SMI. A linear fit ($\Gamma \propto q^2$) of the latex standard gave an $R^2 = 0.993$, while the linear fit for the SMI data gave $R^2 = 0.925$. When fitting the SMI data to an exponential curve ($\Gamma \propto \exp(q^2)$), R^2 increased to 0.975 (Figure 8). The improved fit indicates that a certain fraction of the particles are anisotropic, with the remaining most likely isotropic polymer aggregates.

Concluding Remarks

Association between racemo-di-isotactic SMI polymers was investigated theoretically and the experimental results show rod-shaped aggregates. The bent associations are more stable because of van der Waals interactions between maleimide chains. Multiple bent associations form a minimum-energy nanotube structure. Although only the self-assembly of relatively long

maleimide chains has been studied here, the conclusions apply to other styrene and maleimide copolymers because removing the maleimide chains does not affect the overall geometry of the polymer.[23] Additionally, the chemical structure of maleimide chains can modify the van der Waals interaction.

This study shows that by functionalizing SMA the size of the styrene-based alternating copolymer nanotubes can be changed. The shape of SMI nanotubes remains octagonal, the outer diameter increases from 4.4 to 4.8 nm, the inner diameter decreases from 2.0 to 1.7 nm, and aggregation between SMI nanotubes is not possible. In the sample studied, a very small fraction of the SMI actually self-assembled in nanotubes because polymer chirality occurs randomly, and only a low percentage is actually racemo-di-isotactic. Synthesis of racemo-di-isotactic SMI and their derivatives would be very interesting, if achievable.

Acknowledgment. This research was supported by the National Science and Research Council of Canada. We also thank FPInnovations (Paprican division) for financial support. Thomas D. Lazzara acknowledges the award of a Sigma Xi Grant in Aid of Research.

References and Notes

(1) Carloni, P.; Andreoni, W.; Parrinello, M. *Phys. Rev. Lett.* **1997**, *79* (4), 761–764.
(2) Dai, H. *Nanotube Growth and Characterization*; Springer: Berlin, 2001; pp 29−53.
(3) Fenniri, H.; Mathivanan, P.; Vidale, K. L.; Sherman, D. M.; Hallenga, K.; Wood, K. V.; Stowell, J. G. *J. Am. Chem. Soc.* **2001**, *123* (16), 3854–3855.
(4) Ghadiri, M. R.; Granja, J. R.; Milligan, R. A.; McRee, D. E.; Khazanovich, N. *Nature (London)* **1993**, *366* (6453), 324–327.
(5) Hamley, I. W. *Soft Matter* **2005**, *1* (1), 36–43.
(6) Ho, R.-M.; Chen, C.-K.; Chiang, Y.-W.; Ko, B.-T.; Lin, C.-C. *Adv. Mater.* **2006**, *18* (18), 2355–2358.
(7) Kim, H. S.; Hartgerink, J. D.; Ghadiri, M. R. *J. Am. Chem. Soc.* **1998**, *120* (18), 4417–4424.
(8) Yan, X.; Liu, F.; Li, Z.; Liu, G. *Macromolecules* **2001**, *34* (26), 9112–9116.
(9) Banerjee Ipsita, A.; Yu, L.; Matsui, H. *Proc. Natl. Acad. Sci. U.S.A.* **2003**, *100* (25), 14678–14682.
(10) Djalali, R.; Chen, Y.-f.; Matsui, H. *J. Am. Chem. Soc.* **2003**, *125* (19), 5873–5879.
(11) Reches, M.; Gazit, E. *Science* **2003**, *300* (5619), 625–627.
(12) Ajayan, P. M.; Stephan, O.; Redlich, P.; Colliex, C. *Nature (London)* **1995**, *375* (6532), 564–567.
(13) Tian, Y.; He, Q.; Tao, C.; Cui, Y.; Ai, S.; Li, J. *J. Nanosci. Nanotechnol.* **2006**, *6* (7), 2072–2076.
(14) Blomberg, S.; Ostberg, S.; Harth, E.; Bosman, A. W.; Van Horn, B.; Hawker, C. J. *J. Polym. Sci., Part A: Polym. Chem.* **2002**, *40* (9), 1309–1320.
(15) Chen, Y.; Ji, X.; Jiang, S.; Sun, Q.; Jiang, B. *Colloid Polym. Sci.* **2003**, *281* (4), 386–389.
(16) Luo, Y.; Gu, H. *Polymer* **2007**, *48* (11), 3262–3272.
(17) Wang, M.; Braun, H.-G.; Meyer, E. *Chem. Mater.* **2002**, *14* (11), 4812–4818.
(18) Malardier-Jugroot, C.; van de Ven, T. G. M.; Whitehead, M. A. *Mol. Simul.* **2005**, *31* (2−3), 173–178.
(19) Whitehead, M. A.; Malardier-Jugroot, C.; van de Ven, T. G. M.; Lazzara, T. D. 2005-CA833, 2005118688, **2005**
(20) Harrisson, S.; Wooley, K. L. *Chem. Commun.* **2005**, (26), 3259–3261.
(21) Henry, S. M.; El-Sayed, M. E. H.; Pirie, C. M.; Hoffman, A. S.; Stayton, P. S. *Biomacromolecules* **2006**, *7* (8), 2407–2414.
(22) Malardier-Jugroot, C.; van de Ven, T. G. M.; Whitehead, M. A. *J. Phys. Chem. B* **2005**, *109* (15), 7022–7032.
(23) Lazzara, T. D.; Whitehead, M. A.; van de Ven, T. G. M. *J. Phys. Chem. B* **2008**, *112* (16), 4892–4899.
(24) Goren, M.; Qi, Z. G.; Lennox, R. B. *Chem. Mater.* **2000**, *12* (5), 1222–1228.
(25) Hobza, P.; Kabelac, M.; Sponer, J.; Mejzlik, P.; Vondrasek, J. *J. Comput. Chem.* **1997**, *18* (9), 1136–1150.
(26) Hunter, C. A.; Lawson, K. R.; Perkins, J.; Urch, C. J. *J. Chem. Soc., Perkin Trans. 2* **2001**, (5), 651–669.
(27) Hunter, C. A.; Sanders, J. K. M. *J. Am. Chem. Soc.* **1990**, *112* (14), 5525–34.
(28) Hunter, M. J.; G. W. T.; Schlegel, H. B.; Scuseria, G. E.; Robb, M. A.; Montgomery, J. R. C., J. A., Jr.; Vreven, T.; Kudin, K. N.; J. C. B.; Millam, J. M.; Iyengar, S. S.; Tomasi, J.; Barone, V.; Cossi, B. M. M.; Scalmani, G.; Rega, N.; Petersson, G. A.; Hada, H. N. M.; Ehara, M.; Toyota, K.; Fukuda, R. M.; Ishida, J. H.; Nakajima, T.; Honda, Y.; Kitao, O.; Nakai, H.; Li, M. K., X.; Knox, J. E.; Hratchian, H. P.; Cross, J. B.; Adamo, C.; Gomperts, J. J. R.; Stratmann, R. E.; Yazyev, O.; Austin, A. J.; Pomelli; R. C., C.; Ochterski, J. W.; Ayala, P. Y.; Morokuma, K.; Salvador, G. A. V. P.; Dannenberg, J. J. Zakrzewski, V. G.; Daniels, S. D. A. D.; Strain, M. C. Farkas, O.; Rabuck, D. K. M. A. D.; Raghavachari, K.; Foresman, J. B.; Cui, J. V. O. Q.; Baboul, A. G.; Clifford, S.; Cioslowski, J.; Liu, B. B. S. G.; Liashenko, A.; Piskorz, P.; Komaromi, I.; Fox, R. L. M. D. J.; Keith, T.; Al-Laham, M. A.; Peng, C. Y.; Challacombe, A. N. M.; Gill, P. M. W.; Johnson, B.; Wong, W. C. M. W.; Gonzalez, C.; Pople, J. A. Gaussian 03, Revision B.02, 6.0; Gaussian Inc., Pittsburgh, PA, **2003**.
(29) Pecora, B. J. B. A. R. *Dynamic Light Scattering: with Applications to Chemistry, Biology, and Physics*; Wiley: New York, 1976.

MA800926A